FEBS

Letters

journal homepage: www.FEBSLetters.org

The crystal structure of the amidohydrolase VinJ shows a unique hydrophobic tunnel for its interaction with polyketide substrates

Yuji Shinohara [a], Akimasa Miyanaga [b], Fumitaka Kudo [b], Tadashi Eguchi [a,*]

[a] *Department of Chemistry and Materials Science, Tokyo Institute of Technology, O-okayama, Meguro-ku, Tokyo 152-8551, Japan*
[b] *Department of Chemistry, Tokyo Institute of Technology, O-okayama, Meguro-ku, Tokyo 152-8551, Japan*

ARTICLE INFO

ABSTRACT

VinJ is an amidohydrolase belonging to the serine peptidase family that catalyzes the hydrolysis of the terminal aminoacyl moiety of a polyketide intermediate during the biosynthesis of vicenistatin. Herein, we report the crystal structure of VinJ. VinJ possesses a unique hydrophobic tunnel for the recognition of the polyketide chain moiety of its substrate in the cap domain. Taken together with the results of phylogenetic analysis, our results suggest that VinJ represents a new amidohydrolase family that is different from the known α/β hydrolase type serine peptidases.

1. Introduction

Peptidases cleave peptide bonds in proteins and peptide substrates, and about 2% of the genes present in the genomes of every organism encode for peptidases [1]. These enzymes are widely distributed and are critical to the effective maintenance of a variety of different biological systems such as post-translational proteolysis, as well as playing important roles in physiological processes and cellular protection mechanisms [2]. For example, the signal peptide responsible for sorting proteins during their translocation is removed from the protein by peptidase when the proteins reach their final destination [3]. As for the biosynthesis of ribosomal peptides, a peptidase cleaves off the leader peptide to allow for the generation of the bioactive peptides [4,5]. Thus, peptidases are important and intriguing enzymes that are involved in a wide variety of biological processes. Although the biochemical properties of peptidases have been well characterized, our understanding of the substrate specificities of peptidases has been limited to peptides composed of proteinogenic natural amino acids.

Enzymes belonging to the serine peptidase family recognize characteristic sequences of peptides and catalyze the hydrolysis of amide bonds within these sequences [6]. The crystal structures of serine peptidases such as chymotrypsin, trypsin and subtilisin, have provided valuable mechanistic insights into their reactions. Serine peptidases contain a catalytic triad (i.e., Ser-His-Asp) in their active site. The Ser hydroxy group attacks the carbonyl carbon of an amide moiety of the substrate to generate a tetrahedral oxyanion intermediate. Subsequent protonation of the nitrogen atom triggers the collapse of the intermediate with the release of an amino group containing product and the concomitant formation of an acyl-enzyme species, which undergoes hydrolysis to give a carboxylate-containing product and the active enzyme. In contrast to this conserved catalytic mechanism, the substrate recognition mechanism is diverse. The substrate specificity is basically controlled by the structure of the substrate binding site, including the S1 site adjacent to the catalytic triad [7].

We previously reported that the amidohydrolase VinJ, which belongs to the serine peptidase family, is involved in the biosynthesis of the macrolactam antibiotic vicenistatin, which is produced by *Streptomyces halstedii* HC34 [8]. Vicenistatin contains the unique β-amino acid unit 3-amino-2-methylpropionate at the starter position of its polyketide backbone. This starter unit is biosynthesized from ʟ-glutamate via (2*S*,3*S*)-3-methylaspartate, which is initially transferred onto the standalone acyl carrier protein (ACP) VinL by the ATP-dependent ligase VinN. After decarboxylation with the PLP-dependent enzyme VinO, the resulting 3-aminoisobutyryl
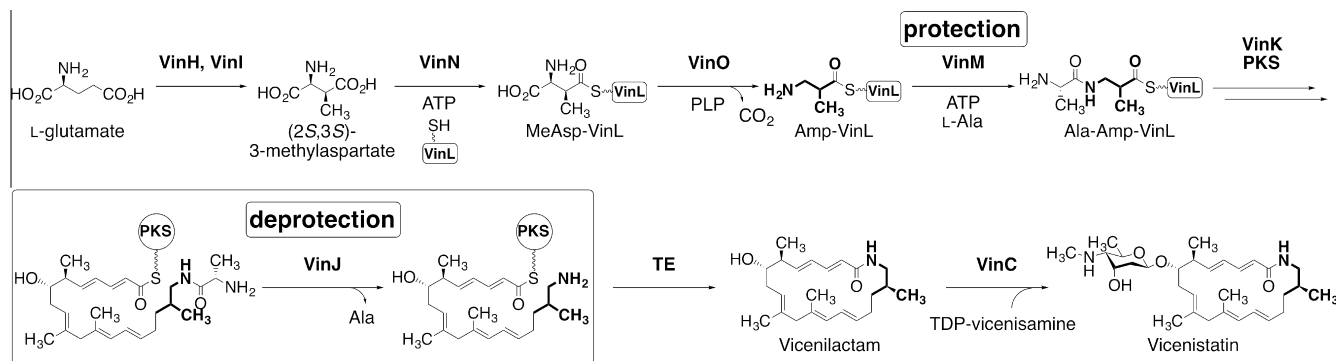
Fig. 1. Biosynthetic pathway of vicenistatin. VinJ catalyzes the hydrolysis of an amide bond in the alanyl-polyketide chain.

moiety is aminoacylated with L-alanine to give L-alanyl-3-aminoiso-butyryl-ACP by the unique ATP-dependent ligase VinM, presumably to avoid spontaneous formation of a six-membered lactam during the elongation of the polyketide chain at module 1 of VinP1. The dipeptide moiety is transferred to the ACP domain of VinP1, which initiates the elongation of the polyketide chain. It has been proposed that polyketide synthases VinP1, P2, P3, and P4 elongate polyketide chains harboring a terminal alanyl moiety, and that this moiety is subsequently hydrolyzed by VinJ prior to the macrolactam forma-tion, which is catalyzed by the thioesterase domain of VinP4 (Fig. 1). We have previously shown that VinJ catalyzes the hydrolytic cleavage of the terminal L-alanyl group from N-alanyl-secovicenilac-tam ethyl ester, which was used to mimic the elongated polyketide substrate attached to ACP [9]. VinJ homologous genes are present in the other gene clusters responsible for the biosynthesis of β-amino acid containing macrolactams, suggesting that VinJ-type amidohy-drolases are commonly used in the biosynthesis of macrolactams [10–14]. Herein, we report the crystal structure of VinJ to determine the structural basis of polyketide substrate recognition. Interest-ingly, VinJ has an unusual hydrophobic tunnel that accommodates the polyketide moiety of the substrate through hydrophobic interactions.

2. Materials and methods

2.1. Preparation of purified VinJ protein

Escherichia coli BL21(DE3) cells harboring a pColdI-*vinJ* plasmid [9] were grown at 37 °C in Luria Bertani broth containing ampicil-lin (50 μg/mL). After the optical density at 600 nm reached 0.6, protein expression was induced by the addition of isopropyl β-D-1-thiogalactopyranoside (0.2 mM), and the cells were then cul-tured for an additional 16 h at 15 °C. The recombinant VinJ protein, which was collected from cell-free extracts prepared by sonication, was purified on a TALON affinity column (Clontech, Mountain View, CA, USA). For the construction of the S110A mutant, the pColdI-*vinJ* plasmid was used for the site-directed mutagenesis. Site-directed mutagenesis was performed with a QuikChange site-directed mutagenesis kit (Stratagene, La Jolla, CA, USA) using the following oligonucleotides: 5′-ctcttcggccaggcctggggcgggat-3′ and its complementary oligonucleotide. The mutation was con-firmed by determining the nucleotide sequence. This plasmid was introduced into *E. coli* BL21(DE3) cells, and the mutated en-zyme was prepared as described above.

2.2. Kinetic analysis of VinJ using N-alanyl-secovicenilactam ethyl ester

N-alanyl-secovicenilactam ethyl ester and secovicenilactam ethyl ester were synthesized as described previously [9]. N-alanyl-secovicenilactam ethyl ester (varied between 1 and 100 μM) was reacted with purified VinJ (1 nM) in a 50 mM Tris buffer (pH 7.5) containing 10% glycerol (100 μL total volume), and the resulting solution was incubated at 28 °C for 10 min before being quenched with ethyl acetate. The reaction product was extracted with ethyl acetate (3 × 100 μL) and the combined organic extracts were evaporated to dryness to give a residue, which was dissolved in methanol (10 μL) and subjected to HPLC analysis. HPLC analysis was performed on a Hitachi HPLC system (Hitachi, Tokyo, Japan) equipped with a L-4000 UV Detector and L-6250 Intelligent Pump, using a Pegasil ODS column (4.6 × 250 mm) (Shenshu Scientific, Tokyo, Japan). Solvents A (0.1% TFA in water) and B (0.1% TFA in acetonitrile) were used as the mobile phases according to the following conditions: 0–20 min, 50% B; 20–25 min, 50–70% B linear gradient; 25–30 min, 70% B. The HPLC analysis was performed with a flow rate of 1.0 mL/min. Each reaction was carried out in tripli-cate. Secovicenilactam ethyl ester was used to generate standard curves for the quantification of the products. Steady-state parame-ters were estimated by fitting the initial velocities calculated from the HPLC-UV detection results to the Michaelis–Menten equation.

2.3. Kinetic analysis of VinJ using L-alanine p-nitroanilide

A continuous spectrophotometric assay using L-alanine p-nitro-anilide (Ala-pNA) was carried out as follows. The reaction was ini-tiated by the addition of VinJ (10 nM) to a mixture containing 50 mM Tris buffer (pH 7.5), 10% glycerol and Ala-pNA (varied be-tween 100 and 4000 μM) (500 μL total volume) at 28 °C, and the increase in absorbance at 405 nm attributable to the release of p-nitroaniline per second was monitored using a UV-2450 spectro-photometer (Shimadzu, Tokyo, Japan). The initial velocity was determined from the linear portion of the optical density profile ($\varepsilon_{405\ nm}$ = 10 600 $M^{-1}cm^{-1}$).

2.4. Crystallization, data collection and structural determination

Crystals of VinJ were grown from a 1:1 (v/v) mixture of a VinJ protein solution [10 mg/mL in 5 mM Tris–HCl (pH 7.5)] and a res-ervoir solution (0.2 M lithium acetate, pH 7.0, 20% polyethylene glycol 3350) using the sitting-drop vapor diffusion method at 5 °C. Prior to the collection of the X-ray data, the crystals were soaked in a reservoir solution containing 25% glycerol as a cryopro-tectant and flash-frozen in a stream of liquid nitrogen. The X-ray diffraction data were collected on a beamline BL-5A at the Photon Factory (Tsukuba, Japan), and were subsequently indexed, inte-grated, and scaled using the iMosflm program [15]. The initial phases were determined by the molecular replacement method using the Molrep program [16], with the crystal structure of the putative proline iminopeptidase *Mycobacterium smegmatis* (PDB code: 3NWO) being used as a search model. The ARP/wARP

program [17] was used for automatic initial protein model building. Coot [18] was used for visual inspection and manual rebuilding of the model. Refmac [19] was used for refinement. The figures were prepared using Pymol [20]. The cavity volumes were calculated using the CASTp program [21]. The resulting coordinates and structure factors have been deposited in the Protein Data Bank (PDB code: 3WMR).

2.5. Docking analysis

The energy-minimized conformation of the *N*-alanyl secovicenilactam thioester was generated by the PRODRG2 Server [22]. The VinJ structure was prepared according to requirements of Auto-Dock v4.2 [23], and a series of docking simulations were performed using the implemented Lamarckian genetic algorithm. The cubic energy grid was centered at the hydrophobic tunnel and had an extension of 60 Å in each direction. Although the methylene moiety of the ligand was treated as being flexible, the olefin moiety of the ligand and all of the protein residues were kept rigid. A total of 256 independent docking runs were performed, and the resulting binding modes were ranked into clusters based on their binding energies.

3. Results and discussion

3.1. Kinetics of the VinJ reaction

Kinetic analysis of VinJ using *N*-alanyl-secovicenilactam ethyl ester revealed that VinJ exhibited comparable kinetic values ($k_{cat} = 8.3 \times 10^3$ s^{-1}, $K_m = 25$ μM and $k_{cat}/K_m = 3.3 \times 10^8$ M^{-1} s^{-1}) to several well-known serine peptidases, including chymotrypsin and trypsin, which hydrolyze peptides with k_{cat}/K_m and k_{cat} values of about 10^7 M^{-1}s^{-1} and 100 s^{-1}, respectively [7]. To evaluate the substrate specificity of VinJ, we also carried out kinetic analysis using the smaller substrate Ala-pNA, which does not contain polyketide chain. As a result, VinJ exhibited a much higher K_m value (2.2 mM). These results indicate that VinJ recognizes the polyketide chain of its substrates. Furthermore, these results suggested that the ACP thioester moiety of the assumed natural biosynthetic intermediate is not necessary for substrate recognition.

3.2. Overall structure of VinJ

To develop a greater insight into the structural basis of the substrate recognition mechanism of VinJ, we determined its crystal structure at a resolution of 1.95 Å (R_{fac}/R_{free} = 16.5/20.6) (Table 1). Three VinJ molecules are present in each crystallographic asymmetric unit. Each crystal contact area observed in the asymmetric unit is less than 500 Å^2, indicating that the areas are too small for them to interact as oligomers. Furthermore, the results of gel-filtration chromatography showed that the VinJ protein exists as a monomer in solution (data not shown).

The VinJ structure adopts a conserved α/β fold (Fig. 2A). VinJ is organized into two separate domains, including a catalytic domain (residues 4–133 and 232–299) and cap domain (134–231). The catalytic domain consists of a central 8-stranded β-sheet flanked by six α-helices, whereas the cap domain consists of five α-helices, which forms an α-helical fold. A search for structurally related proteins using the Dali program [24] revealed that the closest functionally characterized protein is tricon-interacting peptidase F1 (F1) (PDB code: 1XQW, Z score = 42.1, root mean square deviation [rmsd] of 1.5 Å, and sequence identity of 28%), which has been reported to accept hydrophobic peptide substrates consisting of 2–4 amino acid residues [25,26]. VinJ is also structurally similar to several other α/β hydrolase type serine peptidases, including proline

Table 1
Data collection and refinement statistics.

Datasets	VinJ
Data collection statistics	
Wavelength (Å)	1.00
Space group	P1
Unit-cell parameters	
a (Å)	52.87
b (Å)	72.62
c (Å)	75.45
α	114.02
β	98.39
γ	98.50
Resolution (Å)	50.9 – 1.95
(outer shell)	(2.06 – 1.95)
Unique reflections	63 660 (7893)
Completeness (%)	88.8 (75.6)
R_{merge} (%)	4.7 (11.6)
I/σ (I)	13.1 (3.9)
Refinement statistics	
R_{fac} (%)	16.5
R_{free} (%)	20.6
No. of protein atoms	7047
No. of solvent atoms	544

iminopeptidase [27] (PIP) (PDB code: 1AZW, Z score = 24.3, rmsd of 2.9 Å, and sequence identity of 20%) and prolyl aminopeptidase [28] (PAP) (PDB code: 1QTR, Z score = 23.7, rmsd of 3.0 Å, and sequence identity of 18%). Further structural comparison of VinJ with F1 revealed that there are similarities in both their catalytic (Z score = 24.8, rmsd of 1.5 Å, and sequence identity of 26%) and cap domains (Z score = 9.5, rmsd of 1.0 Å, and sequence identity of 31%). A comparison of the structure of VinJ with those of PIP and PAP, however, revealed that only the catalytic domains of these proteins are similar, with no detectable similarities seen in their cap domains.

3.3. Active site and terminal amino acid-binding pocket of VinJ

VinJ contains a catalytic triad (i.e., Ser110, Asp250, and His277), which is located on the inside of its catalytic domain, as expected from its amino acid sequence (Fig. 3). The positioning and orientation of the residues in this triad are almost identical to those of several α/β hydrolase type serine peptidases, including F1. To confirm the function of the Ser110 residue in VinJ, we constructed the S110A mutant and analyzed its activity. The S110A mutant exhibited no activity towards the *N*-alanyl-secovicenilactam ethyl ester, indicating that the Ser110 residue acts as a catalytic nucleophile. The side-chain of Ser110 is not oriented toward His277, but instead interacts with the backbone amide nitrogen of Trp111, which forms an oxyanion hole together with Gly39, as observed in the F1 structure [25]. Two glutamates (Glu219 and Glu251), which are supposed to interact with the β-amino group of the 3-aminoisobutyryl moiety of polyketide substrates, are oriented in a similar manner to those observed in the α/β hydrolase type serine peptidases.

Further structural comparison of VinJ with F1 allowed for the estimation of the S1 pocket site, which is believed to be responsible for the recognition of the terminal alanyl moiety of a substrate by VinJ. The structures of F1 complexes with dipeptides such as Phe-Leu show that F1 has a large hydrophobic S1 pocket (337 Å^3) consisting of several small residues such as Val134 and Thr137 [26]. This large hydrophobic pocket explains the substrate specificity shown by F1, where the enzyme can accept peptides containing a bulky amino acid such as Phe at their *N*-terminal. In contrast, the replacement of some of the smaller residues in F1 with bulky residues, such as Met139 and Trp142 in VinJ, provides a relatively

Fig. 2. Structures of VinJ and F1. (A) Overall structure of VinJ. Helices and loops of the catalytic domain, the β-strands of the catalytic domain, and region of the cap domain are shown in yellow, green, and red, respectively. The tunnel entrance is indicated by the black arrow. The catalytic Ser110 is displayed as a pink stick structure. (B) Structure of the substrate binding site in VinJ. Important residues for the formation of the tunnel, residues for the S1 pocket and catalytic triad are shown in yellow, light blue, and pink sticks, respectively. The docked N-alanyl secovicenilactam thioester is shown as a green stick structure. (C) Structure of substrate binding site in F1. The structure of the complex of F1 with Phe-Leu [26] is shown (PDB ID: 1XQW). Residues involved in the formation of the tunnel, as well as residues for the S1 pocket and catalytic triad are shown as purple, orange, and gray stick structures, respectively. The Phe-Leu ligand is shown as a green stick structure.

Fig. 3. Sequence alignment of VinJ from *S. halstedii* HC34 with other VinJ-like proteins involved in the biosynthesis of macrolactams (CmiM6 from *Streptomyces* sp. MJ635-86F5, BecP from *Streptomyces* sp. DSM 21069, MlaP from *Streptomyces* sp. MP39-85, Strop_2777 from *Streptomyces tropica* CNB-440, and IdnL5 from *Streptomyces.* sp. ML 694-90F3) and F1 from *Thermoplasma acidophilum*. The secondary structural elements of VinJ are indicated by bars above the sequence. The circle, triangle, and asterisk show the polyketide recognition and alanine recognition sites and the catalytic triad, respectively.

small S1 pocket (241 Å³), and the small size of this pocket may be responsible to the observed preference for smaller alanyl substrates. In fact, VinJ exhibited a lower activity (∼1%) towards L-phenylalanine p-nitroanilide (Phe-pNA) than Ala-pNA (data not shown), which indicated that VinJ does not prefer bulky amino acyl substrate. BecP, which shares a 65% sequence identity with VinJ, has been reported to prefer Ala-pNA as a substrate over other amino acyl-pNAs [13]. This result is consistent with the substrate specificity of VinJ.

3.4. Polyketide binding tunnel

VinJ has a long and narrow tunnel that extends from its surface to its active site (Fig. 2B). This tunnel is approximately 16 Å long and is composed predominantly of hydrophobic residues such as Tyr183, Phe197, Phe201, Ile204, and Tyr211, which are located in the cap domain. Based on the size, shape and hydrophobic character of this tunnel, it appears to be suitably equipped to interact with a hydrophobic polyketide chain. To understand the interaction

between a polyketide chain and this tunnel, we attempted to cocrystallize the VinJ S110A mutant with *N*-alanyl secovicenilactam ethyl ester. Unfortunately, however, we were unable to observe any electron density corresponding to this substrate analog. We then conducted a computational docking analysis using *N*-alanyl secovicenilactam thioester as a substrate analog. The docking analysis revealed that most of the polyketide chain moiety (N1 amine to C13) was accommodated in the tunnel, and that the remaining moiety (C14 to C20 thioester) was present on the surface of VinJ. The docking model predicted several hydrophobic interactions with the polyketide C2-C13 region, which does not possess any polar groups. Based on this docking analysis, it was assumed that mostly or fully elongated *N*-alanyl polyketide chain would most likely be a suitable substrate for VinJ, although the exact timing of the hydrolytic removal of the alanine group during the polyketide chain elongation process remains unclear.

A comparison of the structural features of the tunnels of VinJ and F1 revealed that they share the fundamental architecture (Fig. 2C and Fig. 3), in that F1 also has a long hydrophobic tunnel (14 Å) connecting its surface to its active site. Despite this fundamental similarity, a few significant differences were observed between the tunnels in these two enzymes. First, the bulky aromatic residues in VinJ, such as Phe197 and Phe201, are replaced by relatively small aliphatic residues in F1, such as Val192 and Leu196, respectively, which could be responsible for the differences observed in the substrate specificity of these enzymes. The bulky aromatic residues in the VinJ structure allow for the construction of a narrower tunnel (~7 Å diameter) as well as facilitating the formation of effective hydrophobic interactions with the polyketide chain. In contrast, F1 has a wider tunnel, which most likely contributes to its tolerance towards a range of hydrophobic peptides possessing various side-chains. Second, there are significant differences between VinJ and F1 in terms of the residues located on their surfaces near the tunnel entrances. In the VinJ structure, Phe176 and Tyr205 form a hydrophobic cleft on the surface. The docking model suggested that this hydrophobic cleft may provide an additional hydrophobic interaction with the polyketide chain. In F1, these residues are replaced with polar residues such as Gln171 and Glu200. Thus, these differences in the structures provide some understanding of the differences in the substrate specificity of VinJ and F1.

3.5. VinJ represents a new amidohydrolase family

VinJ homologs are present in biosynthetic clusters of other β-amino acid containing macrolactams, such as incednine, cremimycin, salinilactam, and BE-14106 [10–14]. Sequence analysis results suggested that these VinJ-type proteins have a similar hydrophobic tunnel and S1 pocket for the hydrolytic removal of an amino acid from the hydrophobic aminoacyl polyketide chain
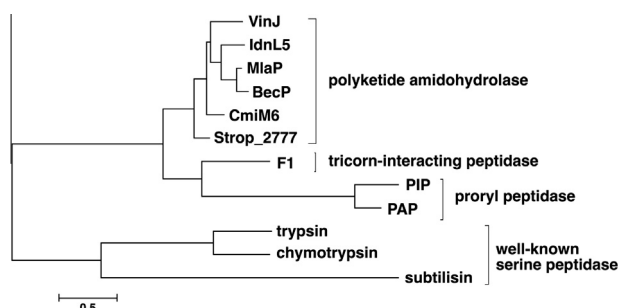
(Fig. 3). Among these VinJ-type proteins, some of the amino acid residues involved in the construction of the hydrophobic tunnel are not conserved. The architecture of the tunnels of the VinJ-type proteins might be slightly different to allow them to effectively accommodate their own polyketide substrate, which possesses distinct starter unit and backbone structure. Phylogenetic analysis showed that these VinJ-type proteins belong to clan SC serine peptidase family based on the MEROPS peptidase classification system [1]. Although VinJ-type proteins are closely related to F1 from a structural perspective, they are classified into phylogenetically distinct groups from F1 (Fig. 4). Thus, VinJ-type proteins comprise a new amidohydrolase family derived from clan SC serine peptidases. This study represents a significant contribution to the expansion of our knowledge of the peptidase family, and provides insight into how peptidases have evolved to gain various substrate specificities.

References

[1] Barrett, A.J., Rawlings, N.D. and O'Brien, E.A. (2001) The MEROPS database as a protease information system. J. Struct. Biol. 134, 95–102.
[2] Polgár, L. (2005) The catalytic triad of serine peptidases. Cell. Mol. Life Sci. 62, 2161–2172.
[3] Paetzel, M., Karla, A., Strynadka, N.C.J. and Dalbey, R.E. (2002) Signal peptidases. Chem. Rev. 102, 4549–4580.
[4] Arnison, P.G., Bibb, M.J., Bierbaum, G., Bowers, A.A., Bugni, T.S., Bulaj, G., Camarero, J.A., Campopiano, D.J., Challis, G.L., Clardy, J., Cotter, P.D., Craik, D.J., Dawson, M., Dittmann, E., Donadio, S., Dorrestein, P.C., Entian, K., Fischbach, M.A., Garavelli, J.S., Göransson, U., Gruber, C.W., Haft, D.H., Hemscheidt, T.K., Hertweck, C., Hill, C., Horswill, A.R., Jaspars, M., Kelly, W.L., Klinman, J.P., Kuipers, O.P., Link, A.J., Liu, W., Marahiel, M.A., Mitchell, D.A., Moll, G.N., Moore, B.S., Müller, R., Nair, S.K., Nes, I.F., Norris, G.E., Olivera, B.M., Onaka, H., Patchett, M.L., Piel, J., Reaney, M.J.T., Rebuffat, S., Ross, R.P., Sahl, H., Schmidt, E.W., Selsted, M.E., Severinov, K., Shen, B., Sivonen, K., Smith, L., Stein, T., Süssmuth, R.D., Tagg, J.R., Tang, G., Truman, A.W., Vederas, J.C., Walsh, C.T., Walton, J.D., Wenzel, S.C., Willey, J.M. and van der Donk, W.A. (2013) Ribosomally synthesized and post-translationally modified peptide natural products: overview and recommendations for a universal nomenclature. Nat. Prod. Rep. 30, 108–160.
[5] Zhang, Q. and Liu, W. (2013) Biosynthesis of thiopeptide antibiotics and their pathway engineering. Nat. Prod. Rep. 30, 218–226.
[6] Page, M.J. and Di Cera, E. (2008) Serine peptidases: classification, structure and function. Cell. Mol. Life Sci. 65, 1220–1236.
[7] Hedstrom, L. (2002) Serine protease mechanism and specificity. Chem. Rev. 102, 4501–4523.
[8] Ogasawara, Y., Katayama, K., Minami, A., Otsuka, M., Eguchi, T. and Kakinuma, K. (2004) Cloning, sequencing, and functional analysis of the biosynthetic gene cluster of macrolactam antibiotic vicenistatin in *Streptomyces halstedii*. Chem. Biol. 11, 79–86.
[9] Shinohara, Y., Kudo, F. and Eguchi, T. (2011) A natural protecting group strategy to carry an amino acid starter. J. Am. Chem. Soc. 133, 18134–18137.
[10] Takaishi, M., Kudo, F. and Eguchi, T. (2012) A unique pathway for the 3-aminobutyrate starter unit from L-glutamate through β-glutamate during biosynthesis of the 24-membered macrolactam antibiotic, incednine. Org. Lett. 14, 4591–4593.
[11] Amagai, K., Takaku, R., Kudo, F. and Eguchi, T. (2013) A unique amino transfer mechanism for constructing the β-amino fatty acid starter unit in the biosynthesis of the macrolactam antibiotic cremimycin. ChemBioChem 14, 1998–2006.
[12] Udwary, D.W., Zeigler, L., Asolkar, R.N., Singan, V., Lapidus, A., Fenical, W., Jensen, P.R. and Moore, B.S. (2007) Genome sequencing reveals complex secondary metabolome in the marine actinomycete *Salinispora tropica*. Proc. Natl. Acad. Sci. USA 104, 10376–10381.
[13] Jørgensen, H., Degnes, K.F., Sletta, H., Fjaervik, E., Dikiy, A., Herfindal, L., Bruheim, P., Klinkenberg, G., Bredholt, H., Nygård, G., Døskeland, S.O., Ellingsen, T.E. and Zotchev, S.B. (2009) Biosynthesis of macrolactam BE-14106 involves two distinct PKS systems and amino acid processing enzymes for generation of the aminoacyl starter unit. Chem. Biol. 16, 1109–1121.

Fig. 4. Phylogenetic tree of VinJ homologs and well-known serine-peptidases. The tree was constructed using MEGA5. The branch lengths are proportional to the sequence divergence and the scale of 0.5 amino acid changes per site is indicated in the bottom left of the figure.

[14] Jørgensen, H., Degnes, K.F., Dikiy, A., Fjaervik, E., Klinkenberg, G. and Zotchev, S.B. (2010) Insights into the evolution of macrolactam biosynthesis through cloning and comparative analysis of the biosynthetic gene cluster for a novel macrocyclic lactam, ML-449. Appl. Environ. Microbiol. 76, 283–293.

[15] A.G.W. Leslie, Recent changes to the MOSFLM package for processing film and image plate data, Joint CCP4 + ESF-EAMCB Newsletter on Protein Crystallography 1992 (No. 26).

[16] Vagin, A. and Teplyakov, A. (2010) Molecular replacement with MOLREP. Acta Crystallogr. D 66, 22–25.

[17] Morris, R.J., Perrakis, A. and Lamzin, V.S. (2002) ARP/wARP and automatic interpretation of protein electron density maps. Acta Crystallogr. D 58, 968–975.

[18] Emsley, P. and Cowtan, K. (2004) Coot: model-building tools for molecular graphics. Acta Crystallogr. D 60, 2126–2132.

[19] Murshudov, G.N., Vagin, A.A. and Dodson, E.J. (1997) Refinement of macromolecular structures by the maximum-likelihood method. Acta Crystallogr. D 53, 240–255.

[20] DeLano, W.L. (2002) The PyMOL Molecular Graphics System, DeLano Scientific LLC, Palo Alto, CA.

[21] Dundas, J., Ouyang, Z., Tseng, J., Binkowski, A., Turpaz, Y. and Liang, J. (2006) CASTp: computed atlas of surface topography of proteins with structural and topographical mapping of functionally annotated residues. Nucleic Acid Res. 34, W116–W118.

[22] Schüttelkopf, A.W. and van Aalten, D.M.F. (2004) PRODRG: a tool for high-throughput crystallography of protein–ligand complexes. Acta Crystallogr. D 60, 1355–1363.

[23] Morris, G.M., Huey, R., Lindstrom, W., Sanner, M.F., Belew, R.K., Goodsell, D.S. and Olson, A.J. (2009) Autodock4 and AutoDockTools4: automated docking with selective receptor flexiblity. J. Comput. Chem. 16, 2785–2791.

[24] Holm, L. and Sander, C. (1995) Dali: a network tool for protein structure comparison. Trends Biochem. Sci. 20, 478–480.

[25] Goettig, P., Groll, M., Kim, J., Huber, R. and Brandstetter, H. (2002) Structures of the tricorn-interacting aminopeptidase F1 with different ligands explain its catalytic mechanism. EMBO J. 21, 5343–5352.

[26] Goettig, P., Brandstetter, H., Groll, M., Göhring, W., Konarev, P.V., Svergun, D.I., Huber, R. and Kim, J. (2005) X-ray snapshots of peptide processing in mutants of tricorn-interacting factor F1 from *Thermoplasma acidophilum*. J. Biol. Chem. 280, 33387–33396.

[27] Medrano, F.J., Alonso, J., García, J.L., Romero, A., Bode, W. and Gomis-Rüth, F.X. (1998) Structure of proline iminopeptidase from *Xanthomonas campestris* pv. citri: a prototype for the prolyl oligopeptidase family. EMBO J. 17, 1–9.

[28] Yoshimoto, T., Kabashima, T., Uchikawa, K., Inoue, T., Tanaka, N., Nakamura, K.T., Tsuru, M. and Ito, K. (1999) Crystal structure of prolyl aminopeptidase from *Serratia marcescens*. J. Biochem. 126, 559–565.